International Journal of Concrete Structures and Materials
Vol.2, No.2, pp. 91~98, December 2008

Long-Term Monitoring and Analysis of a Curved Concrete Box-Girder Bridge

Sungchil Lee,[1] Maria Q. Feng,[2] Seok-Hee Hong,[3] and Young-Soo Chung[4]

(Received October 6, 2008, Revised November 30, 2008, Accepted November 30, 2008)

Abstract : Curved bridges are important components of a highway transportation network for connecting local roads and highways, but very few data have been collected in terms of their field performance. This paper presents two-years monitoring and system identification results of a curved concrete box-girder bridge, the West St. On-Ramp, under ambient traffic excitations. The authors permanently installed accelerometers on the bridge from the beginning of the bridge life. From the ambient vibration data sets collected over the two years, the element stiffness correction factors for the columns, the girder, and boundary springs were identified using the back-propagation neural network. The results showed that the element stiffness values were nearly 10% different from the initial design values. It was also observed that the traffic conditions heavily influence the dynamic characteristics of this curved bridge. Furthermore, a probability distribution model of the element stiffness was established for long-term monitoring and analysis of the bridge stiffness change.

Keywords : long-term monitoring, curved concrete bridge, back-propagation neural network, probability distribution model, acceleration measurement, traffic excitation, modal frequency, element stiffness

1. Introduction

Recent advances in sensor, communication, and computer technologies have made automated monitoring of bridge structures a promising alternative to the traditional visual inspection. In fact, many researchers have studied sensor-based monitoring of bridges, most of which dealt with long-span bridges.[1-3] As for medium- and short-span bridges, studies have focused on straight bridges, but not curved ones.[4,5]

Medium- and short-span curved bridges are inevitable in a modern highway system to connect local roadways to highways in interchanges. It is important to monitor and study the performance of such bridges. Different from long-span bridges whose ambient vibrations are caused by both wind and traffic excitations, medium- and short-span bridges are mainly excited by traffic loads.

Many system identification methods have been proposed for identifying structural dynamic properties based on ambient vibration tests, but they suffer from errors caused by unknown input forces. In reality, different input energy level to excite a bridge results in different dynamic properties, i.e. natural frequency, mode shape, damping ratio. The authors experienced on the WSO that the natural frequencies of the bridge from a braking test and a bumping test were not the same because of the different exciting energy level.[6] Therefore it is important to use ambient vibration data sets under a similar traffic condition when identifying the structural dynamic properties. Since not only the excitation energy level but also the dynamic interactions between traveling vehicles and the bridge, but also the environmental conditions such as the temperature and humidity affect the dynamic properties of bridges, a probability distribution model established by long-term bridge monitoring would provide more information about the change of the bridge structural parameter (such as the stiffness) rather than one point estimation at a specific time during a whole bridge life.

The neural network-based system identification method [7-10] has several advantages compared with conventional system identification methods. It is more capable of indentifying elemental stiffness values based on the partially and incompletely measured mode parameters due to the limited sensor number. Furthermore, it is convenient to use neural networks to parameterize any properties of the structures, such as the effective shear area, as the unknowns to be identified. In contrast to many other system identification methods in which the sensitivity matrix may become unstable especially for complex structural systems, the neural network approach does not require calculation of the sensitivity matrix, and thus can be applied to complex civil engineering structures with less numerical difficulty.

In this paper, the back-propagation neural network was adopted to identify the element stiffness of the WSO using the traffic-induced ambient vibration data selected from the population of

[1]KCI Member, Dept. of Civil & Env. Engineering, University of California Irvine, Irvine, 92697 USA. *E-mail: sungcl@uci.edu*
[2]University of California Irvine, Dept. of Civil & Env. Engineering, Irvine, 92697 USA.
[3]KCI Member, Naekyung Engineering Co., LTD. Anyang 431-060, Korea.
[4]KCI Member, Dept. of Civil Engineering, Chung-Ang University, Ansung 456-756, Korea.

data sets collected during the two years of monitoring. The probability distribution model of the element stiffness was established to account for the uncertainties from environmental conditions.

2. Instrumentation and monitoring system

Collaborating with the California Department of Transportation (Caltrans), the authors installed sensors on a new curved concrete bridge, the West Street On-Ramp (WSO), on Interstate 5 in Anaheim, California, during its construction.[6] The bridge opened to traffic in 2001. As shown in Figs. 1 and 2, this three-span continuous bridge has a single-cell cast-in-place pre-stressed post-tension box girder. The total length of the bridge is 151.33 m with the span lengths of 45.77 m, 60.12 m, and 45.44 m. The radius of curvature is 165.00 m. The bridge is supported by two columns and sliding bearings on both abutments. The sliding bearings allow creep, shrinkage, and thermal expansion or contraction.

The monitoring system installed at the WSO includes 11 force-balance servo-type accelerometers mounted permanently at selected locations on the concrete surface, 10 strain gauges embedded in the concrete, one longitudinal displacement sensor and soil pressure sensor at the abutment. The locations and measurement directions of the accelerometers are shown in Fig. 3, and one of the accelerometers is shown in a photo in Fig. 4. The accelerometers on the superstructure were placed along the centerline of the girder.

The strain sensors were embedded in concrete members of the bridge to measure dynamic strains. Each strain sensor was welded to a dummy reinforcing bar and embedded in concrete during the construction. Figure 5 shows the locations of the strain sensors. The displacement sensor was placed to measure the relative displacement between abutment 1 and the box girder in the longitudinal direction and the soil pressure sensor was embedded in the back of abutment 1.

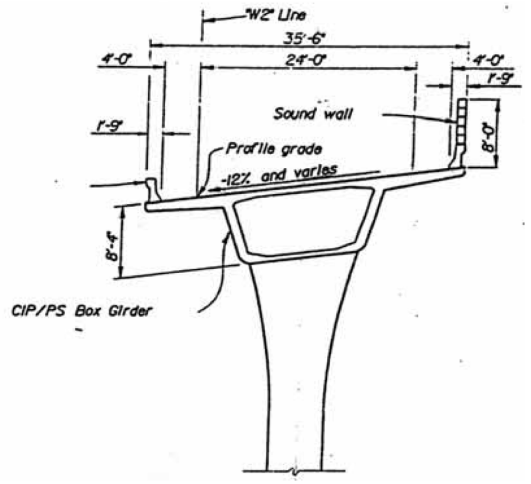

Fig. 1 Typical section of WSO.

Fig. 2 View of WSO.

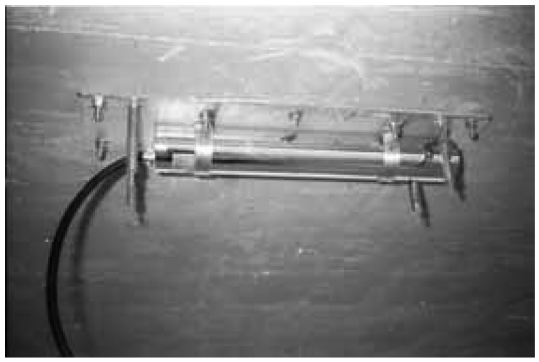

Fig. 3 Installation of accelerometer.

3. Finite element model of WSO

For the purpose of identifying the bridge structural parameters, particularly the stiffness, from the measured dynamic responses to traffic excitations, a 3-dimensional finite element (FE) model of the WSO was developed using the OpenSees program.[11] The bridge was modeled by beam elements, with 200 elements for the deck and 16 elements for each column. The boundary conditions of the finite element model were assumed as fixed for the columns and as springs for the bearings at both of the abutments. The bearing stiffness values were assigned according to the design guidelines,[12] as 9.7×10^5 kN/m, 18.8×10^5 kN/m, and 21.6×10^5 kN/m respectively for the longitudinal, transverse and vertical directions. The rotational spring stiffness values were assigned as 7.5×10^7 kN-m/rad and 4.7×10^7 kN·m/rad respectively along the longitudinal and vertical axes in the horizontal plane. Table 1 summarizes the Young's modulus and the moment of inertia of the column and the deck from the design drawings and Fig. 6 shows the FE model of the WSO.

4. Back-propagation neural network

A back-propagation neural network was developed for identifying the element stiffness of the WSO from the measured dynamic response to traffic excitations. The input of the network are natural frequencies extracted from the measured acceleration responses, while the output of the network are the element stiffness correction factors which are defined as ratios of the identified stiffness and the baseline stiffness. The neural network was trained through finite element analysis.

4.1 Architecture of neural network

As shown in the architecture in Fig. 7, the back-propagation neural network consists of two hidden layers, as well as the input and output layers. Each hidden layer has 10 nodes i.e. neurons. Tangent sigmoid and pure linear functions were used as the trans-

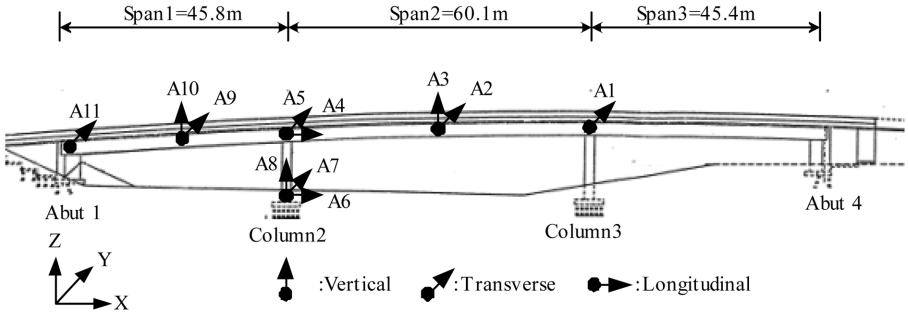

Fig. 4 Layout of accelerometers.

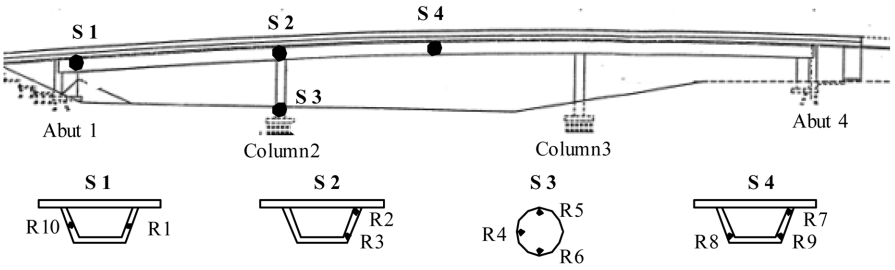

Fig. 5 Layout of strain sensors.

Table 1 Moment of inertia of column and deck element (m^4).

Element	Moment of Inertia		Young's Modulus (MN/m^2)
	I_y	I_z	
Column	2.780	2.780	29,575
Deck	5.472	48.532	26,658

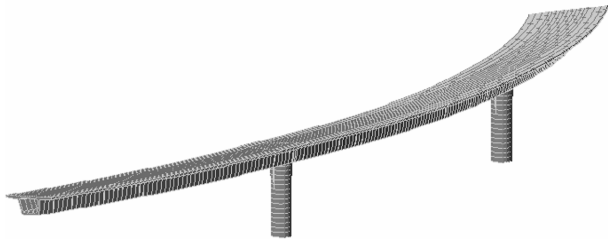

Fig. 6 Finite element model of WSO.

fer function for hidden layers and the output layer, respectively.

Even though the neural network approach can produce stable results for system identification, cautions should be exercised in selecting the input parameters. First of all, the input parameters should be obtained easily and accurately from experiments. Secondly, the input parameters must be sensitive to the output targets. Though the input parameters to the neural network could be any dynamic characteristics of a structure such as mode shapes, mode frequencies, and/or modal damping, the first three mode frequencies were chosen as the input parameters in this study because of the limited number of the installed accelerometers at the bridge and insufficient information regarding the other dynamic properties.

As output parameters, the element stiffness correction factors for the girder, columns, and boundary springs of the WSO were selected. Considering the young age of the bridge, it is assumed that the girder is experiencing a uniform stiffness change along entire girder and so as to each of the columns and abutment soil. In other words, the output of the neural network consists of one stiffness correction factor for the girder, one stiffness correction factor for the column, and one stiffness correction factor of the soil springs at the bridge abutment.

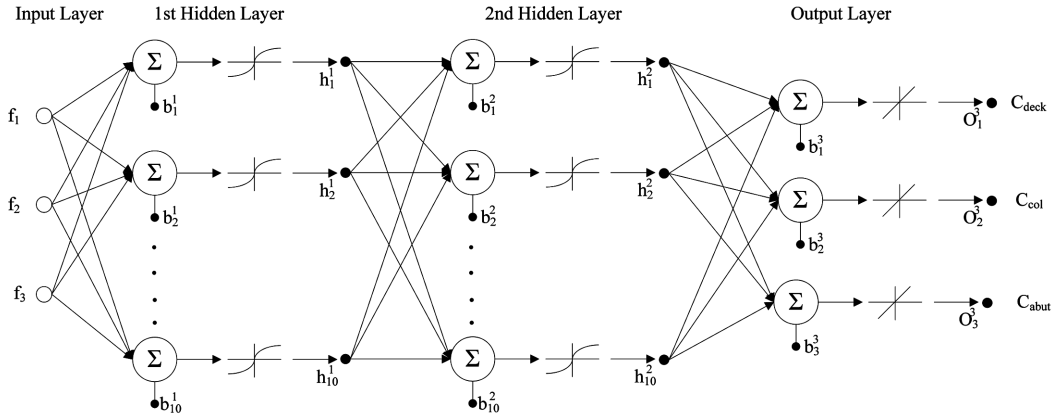

Fig. 7 Architecture of artificial neural network.

4.2 Neural network training process

Training patterns for the neural network were generated through finite element analysis of the bridge using the OpenSees program. For the generation of the training patterns, the correction factors were varied from 0.7 to 1.0 for both the girder and the columns and from 0.5 to 1.0 for the abutment boundary springs. Because of the high uncertainty of the boundary condition, the correction factor of the boundary spring was assumed broader than those of the columns and the girder. For each set of the given correction factors, the corresponding modal frequencies of the bridge model were computed. Table 2 shows examples of the training patterns. In total 4805 training sets were generated. The back-propagation neural network was trained using the Matlab toolbox.[14] To avoid the overfitting problem, an early stopping method was employed. The neural network performance was tested for 30 cases and the results were satisfactory with error of less than 5%.

4.3 Selection of ambient vibration data

As mentioned earlier, the energy level of the traffic excitations affect the dynamic characteristics of a bridge structure. This is demonstrated by an example in Fig. 8, in which power spectral density functions obtained by applying the frequency domain decomposition method[13] from the measured acceleration responses of the WSO. Figures 8 (a) and (b) are based on two different sets of measurement data under different traffic excitation conditions. In Fig. 8 (a) two clear peaks appear around 2.4 Hz and 3.6 Hz and other frequencies between two peaks are suppressed. In Fig. 8 (b), however, the frequencies between 2.5 Hz and 3.5 Hz are predominant. The different frequency characteristics shown in Figs. 8(a) and (b) might have been caused by vehicle-bridge interactions, as well as the different energy levels of the traffic excitations. Obviously using the extracted mode frequencies as the input to the neural network will result in different output results - stiffness correction factors. Therefore, it is important to use the bridge dynamic responses to similar traffic excitations for the purpose of long-term monitoring and identification of the stiffness change. In this study, 20 ambient vibration data sets whose frequency contents are similar to those from the preliminary finite element analysis were selected from the 91 ambient vibration data collected in the two-year monitoring period. By doing so, the bridge response data sets heavily affected by the vehicle-bridge dynamic interactions were avoided.

5. System identification results and probability distribution model

The first three modal natural frequencies of the WSO were extracted from the 20 selected ambient vibration data sets using the frequency decomposition method. Then by inputting into the neural network these modal frequencies, the element stiffness correction factors of the bridge were identified.

Table 2 Training patterns for the WSO.

No	Input (frequency in Hz)			Output (correction factor)		
	1st mode	2nd mode	3rd mode	C_{col}	C_{deck}	C_{bnd}
1	1.751	2.086	2.357	0.700	0.700	0.500
2	1.762	2.128	2.381	0.700	0.700	0.600
...	...	...	...	...	...	...
4805	2.084	2.509	2.819	1.000	1.000	1.000

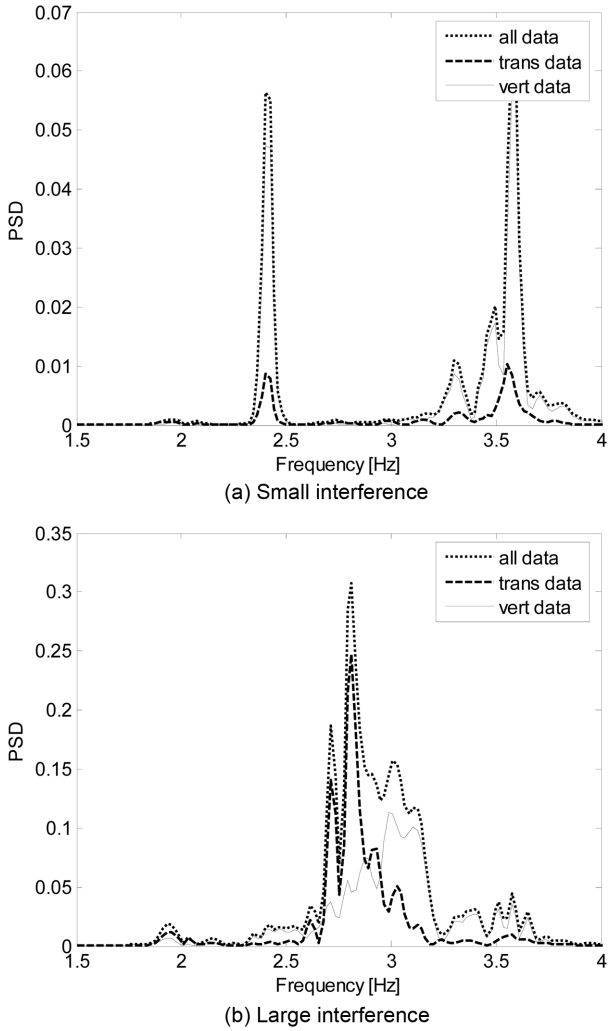

Fig. 8 Power spectral density function from ambient vibration data of WSO.

5.1 Element stiffness correction factor

Table 3 shows the identified element stiffness correction factors over the period of two years. Figure 9 shows the dispersion of the modal frequencies and the element stiffness correction factors. The average values of the element stiffness correction factors are 0.911, 0.903, and 1.107 for the column, the girder, and the boundary soil spring, respectively.

5.2 Probability distribution model of element stiffness

Based on the identified element stiffness from neural network, the probability distribution models for the element stiffness correction factors were established. Figures 10 and 11 show the probability plots of the element stiffness correction factors assuming the normal (Eq.1) and the log-normal distributions (Eq.2), respectively.

$$f_X(x) = \frac{1}{\sigma\sqrt{2\pi}}\exp\left[-\frac{1}{2}\left(\frac{x-\mu}{\sigma}\right)^2\right] \qquad -\infty < x < \infty \qquad (1)$$

$$f_X(x) = \frac{1}{\sqrt{2\pi}\zeta x}\exp\left[-\frac{1}{2}\left(\frac{\ln x-\lambda}{\zeta}\right)^2\right] \qquad 0 \le x < \infty \qquad (2)$$

Table 3 Element stiffness correction factors from neural network.

Date	Input (Hz)			Correction factor		
	First	Second	Third	C_{col}	C_{deck}	C_{bnd}
2004/ 01/30	1.99	2.42	2.79	0.897	0.946	1.150
2004/ 03/30	1.91	2.42	2.75	0.991	0.930	1.168
2004/ 10/21	1.99	2.38	2.77	0.825	0.937	1.112
2004/ 11/03	1.91	2.40	2.59	0.894	0.819	0.959
2004/ 12/16	1.97	2.40	2.71	0.825	0.938	1.070
2005/ 02/ 11	2.03	2.36	2.81	0.892	0.911	1.071
2005/ 03/ 17	1.99	2.41	2.83	1.009	0.850	1.202
2005/ 05/ 17	1.95	2.40	2.73	0.874	0.937	1.148
2005/ 08/ 02	1.93	2.38	2.73	0.903	0.921	1.160
2005/ 09/ 21	1.95	2.40	2.79	0.940	0.923	1.174
2005/ 09/ 23	1.90	2.35	2.72	0.932	0.876	1.180
2005/ 10/ 28	1.99	2.42	2.78	0.884	0.948	1.141
2005/ 11 /22	1.93	2.63	2.71	0.960	0.934	1.153
2005/ 12/ 23	1.97	2.35	2.75	0.796	0.927	1.114
2006/ 01/ 14	1.99	2.42	2.81	0.930	0.933	1.166
2006/ 02/ 03	1.95	2.38	2.77	0.899	0.921	1.168
2006/ 03/ 13	1.99	2.42	2.85	1.158	0.681	1.265
2006/ 03/ 24	1.97	2.42	2.83	1.008	0.873	1.195
2006/ 05/ 08	1.97	2.40	2.75	0.858	0.940	1.138
2006/ 06/ 08	1.97	2.36	2.71	0.771	0.935	1.018
2006/ 09/ 08[1)]	1.90	2.31	2.68	0.812	0.872	1.148
2006/ 09/ 08[2)]	2.01	2.36	2.66	0.988	0.904	0.462
Average	1.96	2.39	2.75	0.911	0.903	1.107

[1)] : Field test -braking test, [2)] : Field test - bumping test

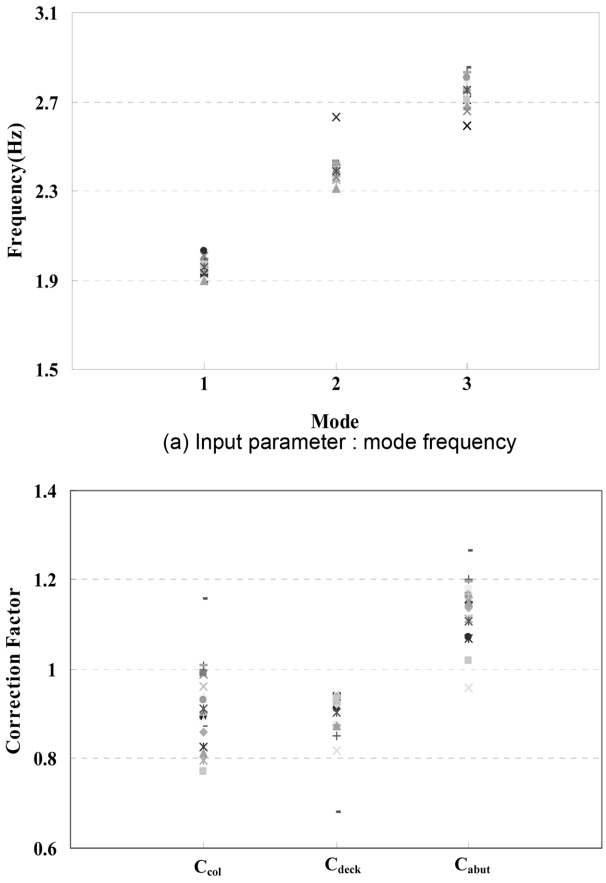

Fig. 9 Input and output parameter of BPNN.

where, X is a random variable, μ and σ are the mean and standard deviation respectively, of the variate, λ and ζ are, respectively, the mean and standard deviation of $\ln(x)$.

For each of the bridge components (i.e., the girder and the column), the normal and the log-normal probability plots show similar results. Since the correction factors cannot be negative values, the log-normal distribution was chosen as the probability distribution model for the element stiffness correction factors.

From Fig. 11, it is observed that all the data fit well with the log-normal distribution for the correction factor of the column, but some data slightly deviate for the girder and boundary spring. Figure 12 shows the log-normal distribution fitting curve and the identified stiffness correction factor of each component. The parameters of the log-normal distribution of each component were calculated from the maximum likelihood estimation and they are shown in Table 4. The mean and standard deviation values of each correction factor in Table 4 were derived by Eq. (3) and (4)

$$\mu = \exp\left(\lambda + \frac{1}{2}\zeta^2\right) \tag{3}$$

$$\sigma^2 = \mu(\exp(\zeta^2)-1) \tag{4}$$

It can be observed from Table 4 that the factor of variance of the boundary spring is much higher than those of the column and the girder. It means that the modal frequencies of the bridge are more sensitive to the stiffness of the boundary soil than the bridge columns and the girder. From the log-normal probability distribution

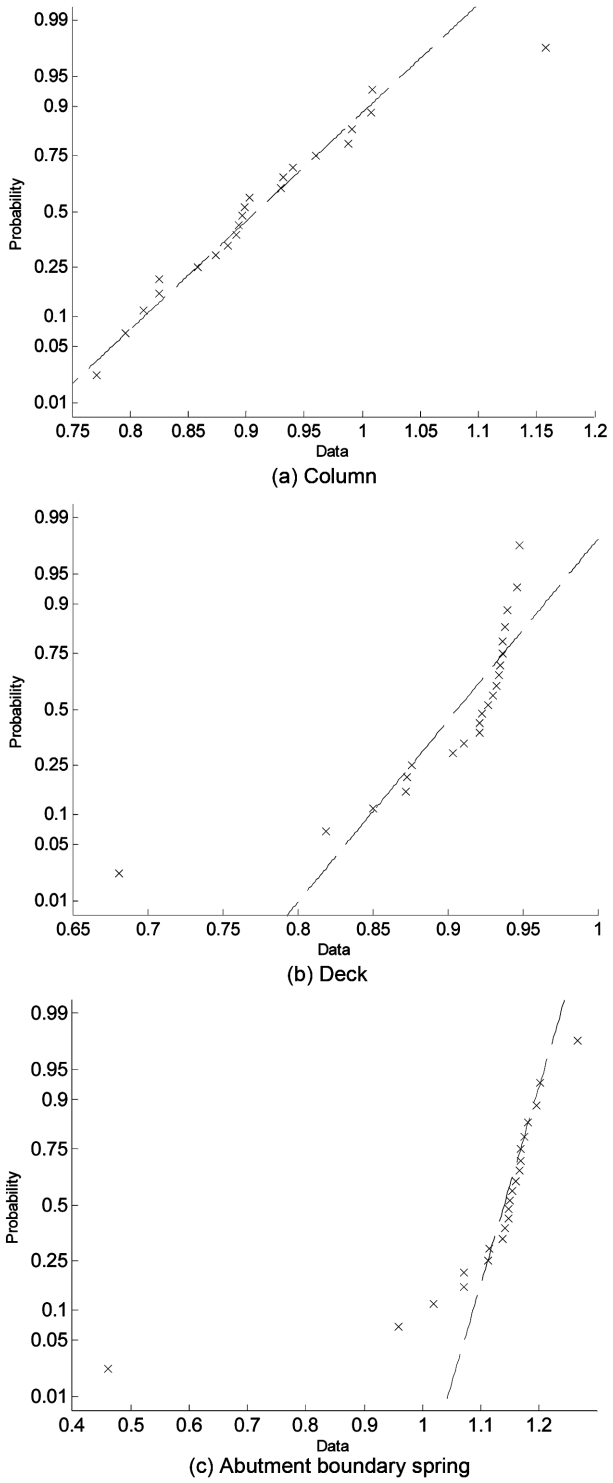

Fig. 10 Probability plot of element stiffness correction factor : Normal distribution.

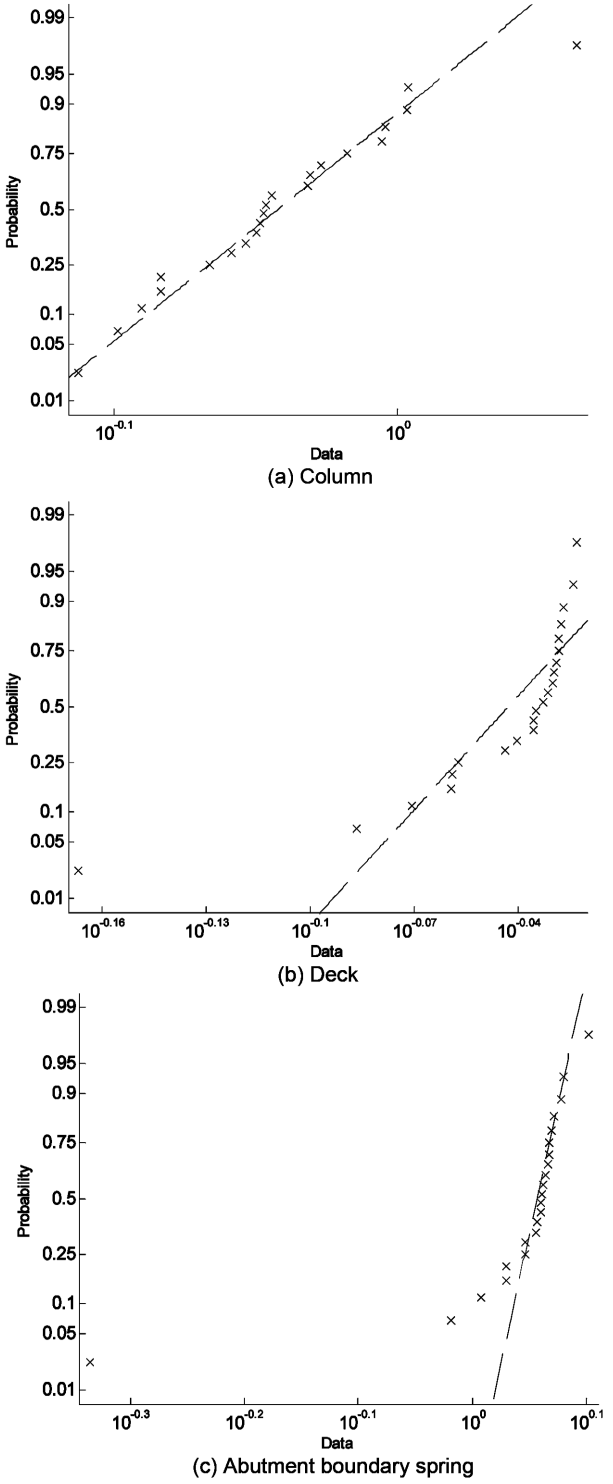

Fig. 11 Probability plot of element stiffness correction factor : Lognormal distribution.

model of the correction factor, the mean of stiffness change from initial design values are found to be −9%, −10%, and +11% for the column, deck and abutment boundary spring stiffness, respectively.

6. Conclusions

From the two-year ambient vibration monitoring data collected

Table 4 Probability parameters of correction factor

Element	$\lambda = E(\ln(X))$	$\zeta = \sqrt{Var(\ln(X))}$	μ	σ	COV
Column	−0.097	0.093	0.911	0.085	0.094
Deck	−0.105	0.073	0.903	0.066	0.073
Boundary spring	0.087	0.201	1.113	0.225	0.203

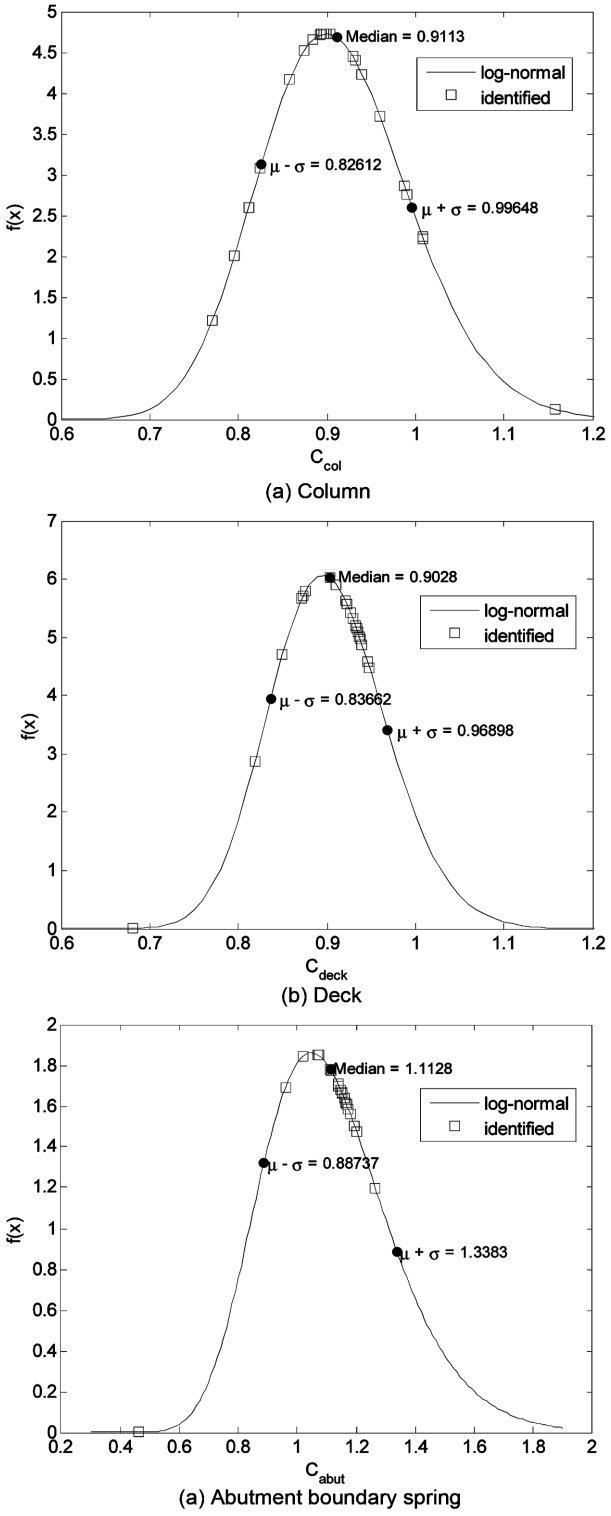

Fig. 12 Log-normal distribution fitting of correction factors.

at the West St. On-Ramp, the change in the stiffness of the columns, the girder, and the boundary spring was identified using a back-propagation neural network. For this curved bridge, it was found that the natural frequencies of the bridge extracted from the measured vibration data were heavily influenced by the vehicle-bridge interactions as well as the energy level of the traffic excitations. For this study, 20 vibration measurement data sets showing similar frequency response patterns were selected from the total 90 data sets. These data sets were considered to be excited by similar traffic conditions and not influenced by the vehicle-bridge interactions.

From the identified element stiffness correction factors, the probability distribution model of the element stiffness was established for the two-year monitoring period under the assumption of the log-normal distribution. The higher factor of variance of the correction factor of the abutment boundary spring indicated that the modal frequencies of the bridge are more sensitive to the abutment soil springs than the bridge columns and girder. In addition, it was found that the identified stiffness values of the columns and the girder were approximately 10% different from the design values.

In the future, the authors will continue collecting and analyzing traffic-induced vibration data from the curved West St. On-Ramp. A long-term trend in the element stiffness change will be traced in the probabilistic framework. In addition, dynamic interactions between traveling vehicles and the bridge structure will be studied, which is believed to play an important role in the dynamic response of a curved bridge.

Acknowledgments

This study was supported by the NaeKyung Engineering Company and the Infra-Structures Assessment Research Center (ISARC) funded by the Ministry of Land, Transport, and Maritime Affairs (MLTM), Korea. The authors gratefully acknowledge this support.

References

1. Shahawy, M. A. and Arockiasamy, M., "Analytical and measured strains in Sunshine Skyway Bridge II," *Journal of Bridge Engineering*, Vol. 1, No. 2, 1996, pp. 87~97.

2. Barrish, R. A. Jr., Grimmelsman, K. A., and Aktan, A. E., "Instrumented monitoring of the Commodore Barry Bride," *Proceedings of SPIE*, No. 3995, 2000, pp. 112~122.

3. Abe, M., Fujino, Y., Yanagihara, M., and Sato, M., "Monitoring of Hakucho Suspension Bridge by Ambient Vibration Measurement," *Proceedings of SPIE*, No.3995, 2000, pp. 237~244

4. Sartor, R. R., Culmo, M. P., and DeWolf, J. T., "Short-term Strain Monitoring of Bridge Structures." *Journal of Bridge Engineering*, Vol. 4, No.3, 1999, pp. 157~164.

5. Choi, S., Park, S., Bolton, R., Stubbs, N., and Sikorsky, C., "Periodic Monitoring of Physical Property Changes in a Concrete Box Girder Bridges." *Journal of Sound and Vibration*, Vol. 278, 2004, pp. 365~381.

6. Feng, M. Q. and Kim, D. K., *Long-Term Structural Performance Monitoring of Two Highway Bridges*, Technical Report of the California Department of Transportation, 2001.

7. Yun, C. B., Yi, J. H., and Bahng, E. Y., "Joint Damage Assessment of Framed Structures Using a Neural Networks Technique." *Engineering Structures*, Vol. 23, No. 5, 2001, pp. 425~435.

8. Masri S., F., Smyth, A. W., Chassiakos, A. G., Caughey, T. K., and Hunter, N. F., "Application of Neural Networks for Detection of Changes in Nonlinear Systems". *Journal of Engineering Mechanics*, Vol. 126, No. 7, 2000, pp. 666~676.

9. Feng, M. Q. and Bahng, E. Y., "Damage Assessment of Jacketed RC Columns Using Vibration Tests," *Journal of Structural Engineering*, Vol. 125, No. 3, 1999, pp. 265~271.

10. Feng, M. Q., Kim, D. K., Yi, J-H and Chen, Y., "Baseline

Models for Bridge Performance Monitoring." *Journal of Engineering Mechanics*, Vol. 130, No. 5, 2004, pp. 562~569.

11. Pacific Earthquake Engineering Research Center, *OpenSees, Reference Manual*, PECCR 2001.

12. Federal Highway Administration, *Seismic Design of Bridges Design Example No.6: Three-span Continuous CIP Concrete Box Bridge*, FHWA, 1996.

13. Brinker, R., Zhang, L., and Andersen, P., "Modal Identification of Output-only System Using Frequency Domain Decomposition." *Smart Material and Structure*, Vol. 10, No. 3, 2001, pp. 441~455.

14. The Mathworks Inc, *Neural Network Toolbox*, 2004.